Contents

Summary

This technical note presents the results of the work aimed at the further development of multi-compartment POP transport model for the EMEP region. The elaboration of this model on the basis of multi-compartment approach was initiated by EMEP/MSC-E several years ago. Its current stage is focused on one of the environmental media considered in the model, namely, the sea water compartment. The previous version of the model included a simplified description of exchange processes between the atmosphere and sea water, which was represented as a well mixed layer of a constant depth. There are a number of scientific studies confirming that oceans play a significant role in global cycling of some persistent organic pollutants (POPs) in the environment. The results of these investigations were used for the modification and refinement of ocean part of POP transport model. Modified model uses multi-layer vertical structure with 15 layers from top to bottom and considers pollutant transport with sea currents, turbulent diffusion, and air-sea exchange processes. Preliminary results obtained show that description of POP redistribution within sea water using the transport processes and turbulent diffusion leads to noticeable increase of POP accumulation in this compartment. These results reflect current understanding that oceans can be an essential storage medium for some of the POPs, e.g. PCBs. Modeling results were compared with observations of PCB concentrations in sea water. Comparison results show reasonable agreement of computed concentrations with available measurements.

I. Modelling long-range transport and deposition of POPs in the European region with emphasis to sea currents

1. *Introduction*

Multi-compartment models of POP long-range transport describe the partitioning and exchange processes of pollutants between such compartments as the atmosphere, soil, vegetation, water bodies. Depending on a model sophistication and calculation scheme its water compartment can involve underground water, rivers, lakes, coastal zones, inland seas, oceans and their regional basins. In global models describing the pollutant transport over the world the ocean is the most capacious unit for POPs [*Wania et al.*, 1998a]. *A.Strand and O.Hov* [1996] believe that about 90% of lindane total amount are in the ocean. Besides in calculations of POP distribution over the environment the effect of sea surface and deep currents on concentration fields obviously should be taken into account [*WMO*, 1997]. The contribution of advective transport to individual system components can be estimated by parameter $\dfrac{U}{L\lambda}$, where U - characteristic motion velocity in the compartment, L - characteristic linear dimension, λ - degradation coefficient of a substance being transported (the inverse value of half-decay). As a rule λ for atmospheric pollutants is by an order of magnitude higher or more than for the ocean. The wind speed in the atmosphere is also by one or two orders of magnitude higher than sea current velocities and characteristic dimensions are comparable. Hence, magnitudes of parameters $\dfrac{U}{L\lambda}$ are close and reasonably safe to suggest that the advective pollutant transport by sea currents is as important as the atmospheric transport. A similar parameter can be suggested for turbulent diffusion: $\dfrac{\sqrt{K/\lambda}}{L}$, where K - turbulent diffusion coefficient. This parameter is identical for the turbulent transport processes in the atmosphere and ocean. In global models the ocean is more inertial unit than the atmosphere. In fact, response time can be estimated by parameter $1/\lambda$ which is in 10-100 times greater for the ocean than for the atmosphere. It means that after ceasing POP emissions the ocean will re-emit in 10-100 times longer than the atmosphere. This fact should be taken into account in tackling the problem of POP emission reduction.

Many papers dedicated to numerical simulation of the global and regional pollutant transport using high spatial resolution are published in recent years. *F.Wania and D.Mackay* [1999], however, mention that there are no models of POP transport dynamics in the ocean for the time being. In order to make adequate description of POP distribution in sea basins it is necessary to consider: dynamic fields of horizontal and vertical current velocities, vertical and horizontal diffusion, water temperature and its salinity. Besides we should consider dynamic re-distribution between POP phases in solution associated with the dissolved organic matter and with suspended particles; sedimentation, flocculation processes, decay and generation of particles in sea water; POP exchange through the air-sea interface and other phenomena.

Multi-compartment model describing POP distribution within the EMEP region (figure 1) involving vast water basins is being developed [*Pekar et al.*, 1999]. This model considers the pollutant transport in the marine environment in a simplified way: the whole water body is represented by a vertically mixed layer of 25 m depth. The horizontal transport and the flux across the lower boundary are not considered. POP flux across the upper surface is described by Liss model [*Liss and Slatter et al.*, 1974] which does not take into account the influence of wind speed. In line with recommendations set forth by EMEP Workshop [*WMO*, 1997] a start has been made on improvement of transport models for the marine environment within the EMEP domain. At present modifications were made only for the open oceanic regions. The transport in the inland seas is described by the above mentioned simplified calculation scheme. This report provides the description of the model and preliminary results of computations for one of PCB congeners - PCB-153.
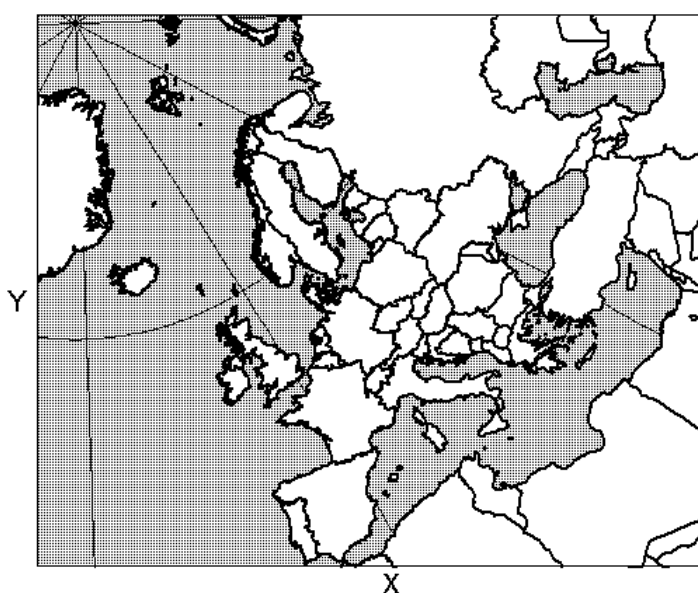
Figure 1.   The EMEP modelling domain

2. *Models considering pollutant transport in the marine environment*

2.1. **Evolutional multi-compartment models**

In this report models describing the dynamics of pollutant behavior in the environment on global and regional scales are discussed. The emphasis is made on models considering pollutant transport in the marine environment.

Evolutional multi-compartment POP transport models are instruments for the evaluation and prediction of concentration dynamics in the air, soil, water and vegetation.

A great number of works are concerned with local models simulating pollution distribution in sea coastal water, harbors, river mouths and inland seas. For example, the paper [*Jilan and Lixian*, 1999] presents the model describing POP dispersion in the bay and tidal events. POP transport in the Caspian Sea from the Volga run-off is considered in [*Ibraev et al.*, 1997]. The authors of the later work use the following transport equation:

$$\partial q / \partial t + v \nabla q + w \partial q / \partial z = 0$$

where $\quad v \nabla = U \dfrac{1}{a \cos \varphi} \dfrac{\partial}{\partial \lambda} + V \dfrac{1}{a} \dfrac{\partial}{\partial \varphi}$,

q - pollutant concentration;

w - vertical velocity;

U – zonal horizontal velocity;

V – meridional horizontal velocity

a - the Earth's radius;

φ - latitude;

λ - longitude.

The model is based on numerical methods with application of the up-wind finite-difference scheme.

Radioactive pollution of the marine environment resulted from nuclear weapon tests, discharge of radioactive wastes and accidents of ships fueled by atomic reactors long ago raised an urgent problem of modelling of radioactive transport in the marine environment. In principle the transport of radionuclides is similar to POP transport except for redistribution processes on organic components of the sea water and pollutant flux through the air-sea interface. A great experience gained in the development of radioactive pollution transport

models with high resolution and their application can be useful for designing similar POP models. Nuclear tests were carried out on Mururua Atoll in the Pacific Ocean in the region of French Polynesia. *L.Alban and R.Jacques* [1999] describe a number of numerical experiments for radionuclides distributions after nuclear tests in this region. The experiment covers the time period of 10 years. The transport equation for the sea pollution has advection and diffusion terms:

$$\partial_t C + \overline{U} \cdot \nabla C = \nabla_h \cdot (A \nabla_h C) + \partial_z K \partial_z C ,$$

where C - concentration;

$\overline{U}$ - velocity vector;

A - horizontal turbulent diffusion coefficient;

K - vertical turbulent diffusion coefficient.

Velocity fields averaged over a year were taken from the global model of ocean circulation [*Guilyardi and Madec*, 1997] with spatial resolution 2° along the longitude, $0.5\text{-}1.7^\circ$ along the latitude and 30 vertical layers (16 layer in the upper 200 m).

R.H.Preller and A.Cheng [1999] described numerical experiments dealing with radioactive contaminant transport in the Arctic and adjacent waters. The calculations covered 10-year periods with different locations and intensities of sources. The following equation for contaminant transport was used:

$$\partial_t T + \overline{U} \cdot \nabla_h T + w \partial_z T = A_{TH} \nabla_h{}^2 T + A_{TZ} \partial_z{}^2 T - \lambda T + \beta T + Source ,$$

where T - pollutant concentration;

$\overline{U}$ - horizontal velocity vector;

w - vertical velocity;

A_{TH} - horizontal turbulent diffusion coefficient;

A_{TZ} - vertical turbulent diffusion coefficient;

λ - pollutant degradation index;

β - river outflow rate of radioactive pollutants (estimated according to river run-off);

Source - source intensity of *T*.

Turbulent diffusion coefficient values were taken as follows: $A_{TH} = 10^7$ cm^2/s, $A_{TZ} = 1$cm^2/s.

Resolution of computational grid was 0.28° along the horizontal with 360x360 knots. Along the vertical there were 15 levels and the upper layer was 30 m deep. The calculation results pointed out that when sources were located in the Kara and Barents seas the maximum concentration in the remote regions of the calculation grid (Alaska coastal line, the northern Atlantic) was observed in 10-15 years after the source emission started.

One-dimensional dispersion of radioactive pollutant along the vertical in the dissolved form and bound to suspended particulate matter was considered in [*Perianez*, 1998b]. A stationary problem of particle distribution with the depth was solved by the equation:

$$K_z \frac{\partial m}{\partial z} = -w_z m \,,$$

where K_z, m and w_z - vertical diffusion coefficient, particle concentration and particle sedimentation velocity respectively.

Particle sedimentation velocity was calculated from Stokes law:

$$w_z = \frac{g(\rho_s - \rho_z)d^2}{12\mu} \,,$$

where g – acceleration of gravity;

μ - water viscosity;

d - mean particle diameter;

ρ_s - particle density;

ρ_z - water density at the depth z.

It is assumed that K_z coefficient is proportional to the horizontal velocity at the depth z:

$$K_z = \alpha\, U_z$$

For a combined solution of the problems of dynamics of radionuclides in the dissolved form and bound to particles the following equations were suggested:

$$\frac{\partial C_d}{\partial t} = \frac{\partial}{\partial z}(K_z \frac{\partial C_d}{\partial z}) - k_1 C_d + k_2 m C_s - \lambda C_d$$

$$\frac{\partial C_s}{\partial t} = k_1 \frac{C_d}{m} - k_2 C_s - \frac{\partial}{\partial z}(w_z C) - \lambda C_s$$

Here C_d - dissolved phase concentration;

C_s - particle phase concentration;

k_1, k_2 - kinetic coefficients;

λ - decay constant.

The radioactive transport simulation in coastal zones with a description of tidal processes is given in [*Perianez and Reguera*, 1999] and in [*Perianez*, 1998a]. In the paper [*Perianez and Reguera*, 1999] dynamics of contaminants in the coastal zone with approximations for shallow water is considered. Two-dimensional equation together with continuity equation is presented as:

$$\frac{\partial HC}{\partial t} + \frac{\partial uHC}{\partial x} + \frac{\partial vHC}{\partial y} = \frac{\partial}{\partial x}(HK_x \frac{\partial C}{\partial x}) + \frac{\partial}{\partial y}(HK_y \frac{\partial C}{\partial y}) - \lambda HC ,$$

where $H = D + z$;

   D - mean sea level;

   C - contaminant concentration;

   u, v - horizontal velocity components;

   K_x, K_y - horizontal turbulent diffusion coefficients along x and y axes respectively;

   λ - contaminant degradation rate.

Three-dimensional equation of advection-diffusion of pollutant is considered in [*Perianez*, 1998a]:

$$\frac{\partial C}{\partial t} + u\frac{\partial C}{\partial x} + v\frac{\partial C}{\partial y} + w\frac{\partial C}{\partial z} = \frac{\partial}{\partial x}(K_h \frac{\partial C}{\partial x}) + \frac{\partial}{\partial y}(K_h \frac{\partial C}{\partial y}) + \frac{\partial}{\partial z}(K_v \frac{\partial C}{\partial z}) - \lambda C ,$$

where K_h - horizontal turbulent diffusion coefficient;

   K_v - vertical turbulent diffusion coefficient;

   C - contaminant concentration;

   λ - contaminant degradation rate;

   u, v, w - velocity components.

Tidal events were considered in calculations of velocities using the continuity equation:

$$\frac{\partial \varsigma}{\partial t} + \frac{\partial}{\partial x}\int_{-h}^{\varsigma} u dz + \frac{\partial}{\partial y}\int_{-h}^{\varsigma} v dz = 0 ,$$

where   h - depth of the undisturbed surface water;

   ς - height of tidal surface disturbances.

A brief review of current transport models for the marine environment leads to the following conclusions: for the development of POP transport in the EMEP marine basin we can use modelling results of radioactive pollutant transport in the ocean described, for example in [*Guilyardi and Madec*, 1997; *Preller and Cheng*, 1999]. In these papers spatial and temporal characteristics are similar to those considered in the problem in question. Processes of advective transport and turbulent diffusion for POP and radionuclides are obviously similar. However, models of interactions of the dissolved phase of pollutants with those in other phases (gas-phase, pollutants associated with particles and dissolved organic matter) will be essentially different. The parameterization of turbulent diffusion on the coastal zones can be made taking into account the results of investigation described in [*Perianez and Reguera*, 1999; *Perianez*, 1998a].

2.2. POP exchange across the air - sea interface

According to some estimations [*Duce*, 1997; *Wania et al.*, 1998a] about 90% of POP enters the ocean through the air-water interface. Similar estimates were made for the Polar ocean [*Macdonald et al.*, 1999]. Obviously in this case an accurate description of POP exchange between air and water compartments is very important. The classical model of a flux through the medium interface with two molecular films on each medium side is considered in the paper [*Liss and Slater*, 1974].

In the paper [*von Hobe et al.*, 1999] carbonyl sulphide transfer through the sea surface is described. The flux through the surface is given according to [*Liss and Slater*, 1974]:

$$F = k_w (c_w - c_a / H),$$

where c_w - water concentration of substance;

   c_a - air concentration of substance;

   k_w - mass transfer coefficient;

   H - Henry's law constant.

k_w values (cm/h) depend on wind speed u (m/s) at 10 m height:

$$k_w = 0.17u \, (Sc/600)^{-2/3} \qquad\qquad \text{at } u <= 3.6;$$
$$k_w = (2.85u - 10.26) \, (Sc/600)^{-1/2} + 0.612 \, (Sc/600)^{-2/3} \qquad \text{at } 3.6 < u <= 13;$$
$$k_w = (5.9u - 49.91) \, (Sc/600)^{-1/2} + 0.612 \, (Sc/600)^{-2/3} \qquad \text{at u > 13.}$$

where Sc - Schmidt number.

On the sea surface diffusion exchange of POP gas-phase, deposition of POP washed out by precipitation in the gas-phase, wet and dry deposition of POP associated with particles take place. According to estimates obtained in [*GESAMP*, 1989] 50-85% of organochloride flux from the atmosphere to the ocean is accounted for the gaseous flux. The gas-phase flux through the water-air interface can be described as [*Liss and Merlivat*, 1986]:

$$F = k_{tot-w} (c_w - c_a / K_{aw}),$$

where k_{tot-w} - total mass transfer coefficient;

   c_w - pollutant concentration in water;

   c_a - pollutant concentration in the air;

   K_{aw} - Henry's law constant.

According to the two-dimensional model of diffusion through the air-water boundary for k_{tot-w} we have:

$$1/\, k_{tot\text{-}w} = 1/\, k_w + 1/\, k_a K_{aw},$$

where k_w value is expressed via the molecular diffusion coefficient in water D_w and surface molecular film thickness Z_w: $k_w = D_w/Z_w$; k_a via similar parameters for the air: $k_a = D_a/Z_a$

More detailed consideration of $k_{tot\text{-}w}$ dependence on wind speed is given in [*Schwarzenbach et al.*, 1993], the results of field experiments of this dependence are discussed in [*Bidleman and McConnell*, 1995]. $k_{tot\text{-}w}$ value depends on temperature in a rather complicated way but in general $k_{tot\text{-}w}$ increases with temperature increase.

Besides POPs transfer through the sea surface with water sprays [*Waldichuck*, 1982] and foam [*Sergeev et al.*, 1979] generated on the surface at wind speed exceeding 3 m/s. The role of water sprays produced on the surface at heavy rain is considered in [*Green and Houk*, 1979], where it is stated that in this case spray formation intensity is comparable with spray formation intensity resulted from wind.

Yu.Sergeev et al. [1979] describe wind velocity effect at 10 m height W_{10} on such transport parameters as molecular surface film thickness, the sea surface area increase due to waves and the surface share covered with foam. For the surface film thickness the following dependence is suggested:

$$\delta = 5.45\,(W_{10})^2 - 1.33\,W_{10} + 900 \qquad \text{at} \qquad W_{10} < 8;$$
$$\delta = 1.83\,(W_{10})^2 - 66\,W_{10} + 583 \qquad \text{at} \qquad 8 <= W_{10} <= 14;$$
$$\delta = 1153\,\exp(-0.263\,W_{10}) \qquad \text{at} \qquad W_{10} > 14,$$

where δ is given in 10^{-6} m, W_{10} in m/s.

For the sea surface area increase coefficient:

$$\alpha_1 = 1 \qquad \text{at} \qquad W_{10} <= 0.5;$$
$$\alpha_1 = 1.35 \qquad \text{at} \qquad 0.5 < W_{10} <= 5;$$
$$\alpha_1 = 1.55 \qquad \text{at} \qquad 5 < W_{10} <= 11;$$
$$\alpha_1 = 1.75 \qquad \text{at} \qquad W_{10} > 11.$$

The coefficient of sea surface area covered with the foam:

$$\alpha_2 = 0 \qquad \text{at} \qquad W_{10} <= 5;$$
$$\alpha_2 = 0.001\,(0.55\,(W_{10})^2 - 1.89\,W_{10} + 1.73) \qquad \text{at} \qquad W_{10} > 5.$$

In the northern regions at low temperatures vast areas are covered with ice. The ice cover appreciably reduces POP flux from the air to the water and backwards [*Macdonald et al.*,

---

1990; *Wania et al.,* 1998b]. At the air-ice or air-snow interface POP exchange processes go on but they are described by other relationships than at the air-water interface. It is worth noting that these processes are poorly studied for the time being. Considering large-scale transport processes it is necessary to take into account the pollutant transport with drifting ice [*Prifman*, 1995] and POP input to the water with melting ice.

2.3. Sedimentation processes in sea water

The sea water is characterized by two phases with which dissolved POPs can be associated: dissolved organic carbon (DOC) representing an aggregate of dissolved organic polymers, colloid formations and other matter which does not deposits on filters, and particulate organic carbon (POC) consisting mainly of algae, bacteria and detritus. Total organic carbon in water is designated as TOC [*GESAMP*, 1989]. To quantify the partitioning of POPs between the dissolved and sorbed phases, the particulate-water equilibrium partition coefficient is introduced:

$$K_d = C_p / C_w,$$

where C_p (mol/kg) - POP concentration per particle mass unit;
C_w (mol/l) - dissolved POP concentration in water.

The capability of POPs to be bound with various organic species available on particles is commonly characterized by the particulate organic carbon partition coefficient:

$$K_{oc} = C_{oc} / C_w,$$

where C_{oc} (mol/kg) - POP concentration per particulate organic carbon mass unit.

K_{oc} values are close for various organic species [*Wania et al.*, 1998b]. K_d and K_{oc} values are related as follows:

$$K_d = K_{oc} \cdot f_{oc},$$

where f_{oc} - organic carbon content in particle mass unit.

To characterize POP binding with dissolved organic compounds DOC-water partition coefficient is introduced:

$$K_{doc} = C_{doc} / C_w,$$

where C_{doc} (mol/kg) - POP concentration per dissolved organic carbon mass unit.

For many sea regions DOC mass in a water volume unit is about 90% of TOC [*GESAMP*, 1989]. It emphasizes the importance of investigating the processes of POP interactions with dissolved organic carbon.

Pollutants associated with particulate organic matter settled out by gravity. The pollutant flux with settling out particles can be expressed by relationship:

$$N_p = C_p \, C_{part} \, V_p,$$

where C_{part} - particle concentration in water;

V_p - particle sedimentation velocity.

Assuming that particles are of a spherical form V_p can be calculated from the Stokes formula. In coastal zones and in river mouths processes opposite to sedimentation (particle resuspension caused by currents, wave or tidal phenomena) can take place.

In the marine environment there are particles of different diameters from 0.1 μm for bacteria to 100 μm for phytoplankton [*Wallberg and Andersson*, 1999]. Particle size distribution depends on many factors. Particles with smaller diameter as a result of collisions flocculate with time [*Gonzalez and Hill*, 1998]. A reverse process - decay and/or dissolving of particles can take place as well.

3.   *Basic equations for POP transport in the marine environment*

In the suggested POP transport model the following physical processes are considered:

- exchange at the air-water interface,
- advective transport by sea currents,
- horizontal and vertical turbulent diffusion,
- POP degradation.

Pollutant vertical transport is rather non-uniform in the ocean. The upper mixed layer with the depth from several tens to several hundreds meters is characterized by strong vertical turbulent mixing. Deep layers, as a rule, are stratified and the vertical turbulent exchange is weaker there. Bearing this in mind for advection-diffusion processes the following equations can be used:

$$\frac{\partial C}{\partial t} + u\frac{\partial C}{\partial x} + v\frac{\partial C}{\partial y} + w\frac{\partial C}{\partial z} = D_H\left(\frac{\partial^2 C}{\partial x^2} + \frac{\partial^2 C}{\partial y^2}\right) + \frac{\partial}{\partial z}\left(D_V(z)\frac{\partial C}{\partial z}\right) - \lambda C \qquad (1)$$

where $D_V(z) = D_{VU}$ at $z <= h$, $D_V(z)=D_{VD}$ at $z > h$, $D_{VU} >> D_{VD}$.

D_{VU} - vertical turbulent diffusion coefficient for the upper mixed layer;

D_{VD} - vertical turbulent diffusion coefficient for deep layers;

h - upper mixed layer depth;

D_H - horizontal turbulent diffusion coefficient;

C - POP concentration in water;

(u, v, w) – x, y, z components of prescribed velocity field;

λ - POP degradation rate.

On the upper oceanic surface POP flux is determined from:

$$F_S = PC_{pr} + \alpha_1(C_a/H - S)((1-\alpha_2)D_\mu/\delta + \alpha_2 H \dot{h}_f),$$

where P- precipitation intensity;

C_{pr} - pollution concentration in precipitation;

C_a - POP concentration in the lower atmospheric layer (on the reference level);

S - POP concentration in the upper water layer;

H - Henry's law constant;

$\alpha_1 = \alpha_1(W)$ - sea surface area increase coefficient dependent on wind speed module;

$\alpha_2 = \alpha_2(W)$ - coefficient of the ratio between the surface area covered with foam to the total surface area;

$\delta = \delta(W)$ - molecular layer depth near the water surface;

W - wind speed module on the reference level;

D_μ - coefficient of molecular diffusion in water;

$\dot{h}_f$ - foam layer thickness reduction rate on the sea surface;

Values of $\alpha_1(W)$, $\alpha_2(W)$, $\delta(W)$, $\dot{h}_f$ are given in [*Sergeev et al*., 1979], D_μ value is given in *M.Pekar et al*. [1998]; P, S, C_{pr}, C_a, W - variables of the experiment.

Boundary conditions are prescribed as follows:

$(\partial C / \partial n)|_{(x,y,z)\in\Gamma} = 0$ on the bottom and coast,

$C|_{(x,y,z)\in\Gamma} = C^B(x,y,z,t)$ at water boundaries,

where $C^B(x, y, z, t)$ - assumed boundary concentration.

The initial condition for POP concentration is prescribed by a defined function C^0:

$C(x, y, z, 0) = C^0(x, y, z)$.

Equation (1) with boundary conditions was solved together with the equation for POP airborne transport in the atmosphere [*Pekar et al*., 1999] by numerical methods. For equation (1) an explicit scheme with splitting by physical processes was used. Advective transport was calculated by up-wind scheme. For the layers in the upper mixed layer an additional mixing step along the vertical was made.

4.   *Numerical experiments*

Numerical experiments using POP transport multi-compartment model with the integrated module of the pollution transport in the marine environment have been carried out for PCB-153. The parameters of the stereographic projection of the calculation grid covering the EMEP domain are as follows: along the horizontal (45x37) with grid cell size 150x150 km, along the vertical for the ocean - 15 layers with depths: 0 m, 25 m, 50 m, 80 m, 130 m, 200 m, 300 m, 450 m, 650 m, 900 m, 1200 m, 1600 m, 2200 m, 3000 m, 4000 m, 5200 m respectively. The velocity fields and the upper mixed layer thickness were defined for every two days with linear interpolation of values obtained within this period of time. Sea current velocities were calculated in Hydrometcentre of Russia by the ocean general circulation model (OGCM). A concise description of the model and calculations of current velocity fields is given in section (II) of this report. For the numerical experiment the following parameters of the model were chosen:

- horizontal turbulent diffusion coefficient 10^3 m^2/s;

- vertical turbulent diffusion coefficient 10^{-4} m^2/s;

- molecular layer thickness near the water surface:
  $\delta(W_{10}) = \delta_0 \cdot \exp(-0.15 \cdot W_{10})$, $\delta_0 = 4 \cdot 10^{-5}$ m, (W_{10} - wind velocity, m/s);

- sea surface area increase due to waves:
  $\alpha_1 = 1.75 - 0.75 \cdot \exp(-0.18 \cdot W_{10})$;

- coefficient of the sea surface covered with foam:
  $\alpha_2 = 1 - \exp(-0.01 \cdot W_{10})$;

- foam thickness decrease rate:
  $h_f = 0.008$ m/s.

Physical-chemical properties of PCB-153 were taken from [*Pekar et al*., 1998].

Zero concentrations in sea water were chosen as initial value. Boundary conditions were chosen the follows: 0.01 ng/m^3 for the Atlantic ocean (left lower corner of the EMEP grid) and zero concentration for the Arctic region (upper left corner of the EMEP grid).

This work presents the results of two experiments with the multi-compartment POP transport model for one-layer stationary ocean (OSO) used in previous version of the model and multi-layer dynamic ocean (MDO) described in this report. In the experiment with OSO we used the transport unit describing the pollutant distribution in the marine environment represented by a motionless water layer of 25 m depth with zero flux outside the layer and a simplified description of the pollutant flux through the sea surface.

The model spin-up was made during 19 years for synoptic parameters of 1996. The results are presented for the 20-th year of the simulation period.

Figure 2 demonstrates the results of the OSO model. Figure 3 shows PCB-153 concentration in the surface ocean layer in the MDO model experiment. The comparison of the two fields of concentrations points out that the introduction of POP transport mechanisms in sea water changes appreciably PCB-153 surface concentration. The maximum concentration observed in the North Sea near the emission sources decreases in the MDO experiment. The concentration difference field in the upper ocean layer for both experiments (figure 4) shows that for the major part of the Atlantic ocean (the central part) with the introduction of transport mechanisms (advection and turbulent diffusion) PCB-153 concentration in the upper layer is decreased. The greatest variations of concentrations (about 50% on average) compared with OSO are observed in the North Sea region. Detailed concentration redistribution for the North Sea and other coastal seas is not discussed here because of rough spatial resolution and insufficient accuracy of calculations of sea currents in these regions.

It is interesting to assess the contribution of sea currents (advection transport) to variation of POP concentration field in the upper ocean layer in comparison with other transport mechanisms (turbulent diffusion, water layer depth variation, modification of POP transport through the sea surface). For this purpose an additional experiment has been carried out with the new model using zero current velocity (MDO0). Surface layer concentration field variation resulted from the introduction of advective transport is demonstrated on figure 5.
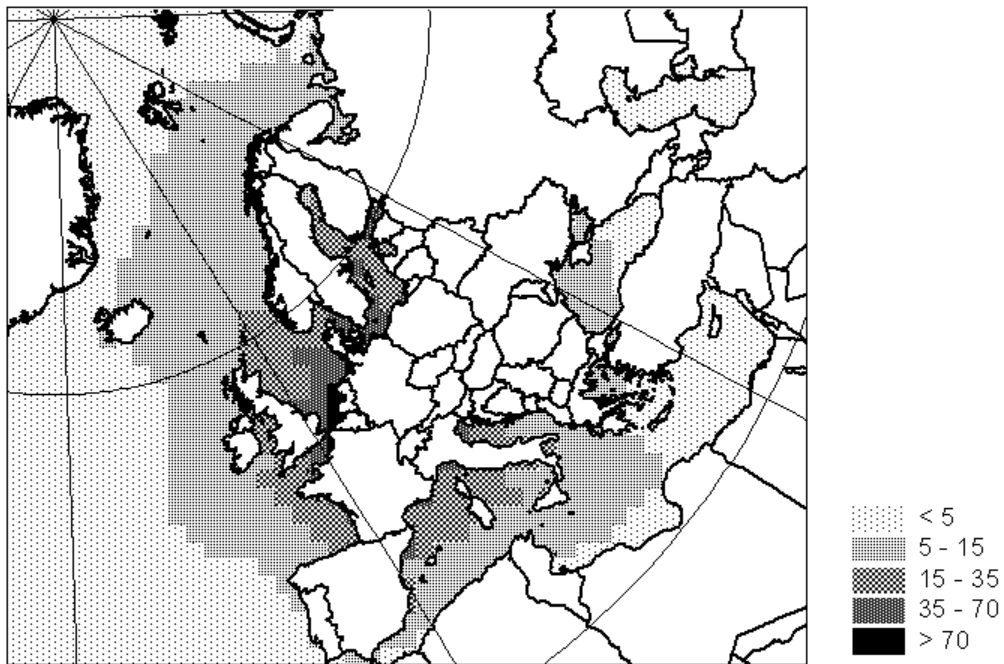
Figure 2. Concentrations of PCB-153 in the upper ocean layer obtained with OSO model, ng/m^3
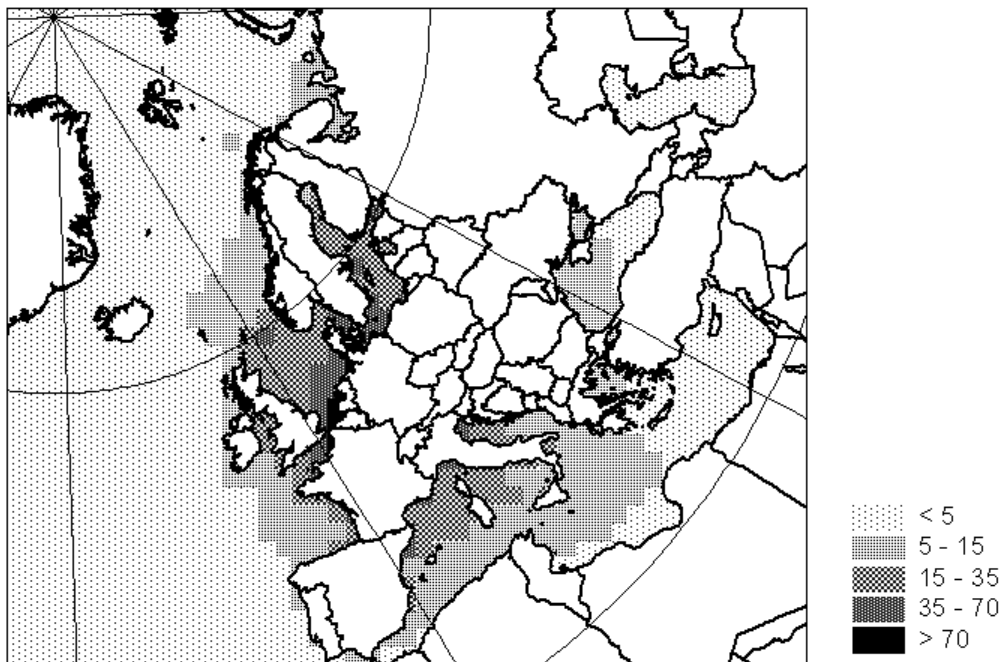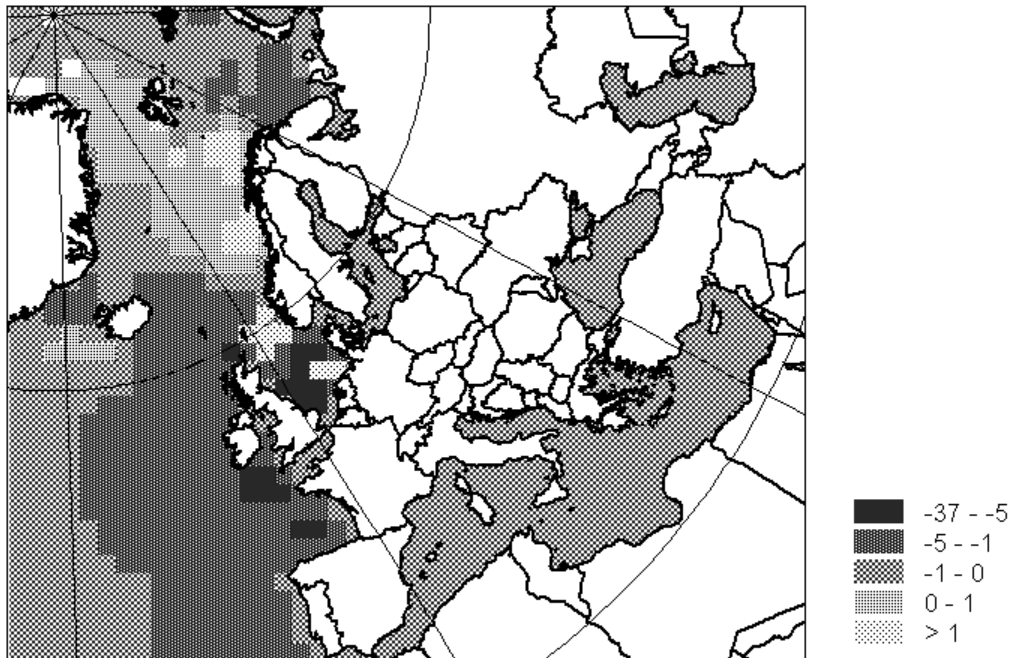

Figure 3. Concentrations of PCB-153 in the upper ocean layer obtained with MDO model, ng/m^3
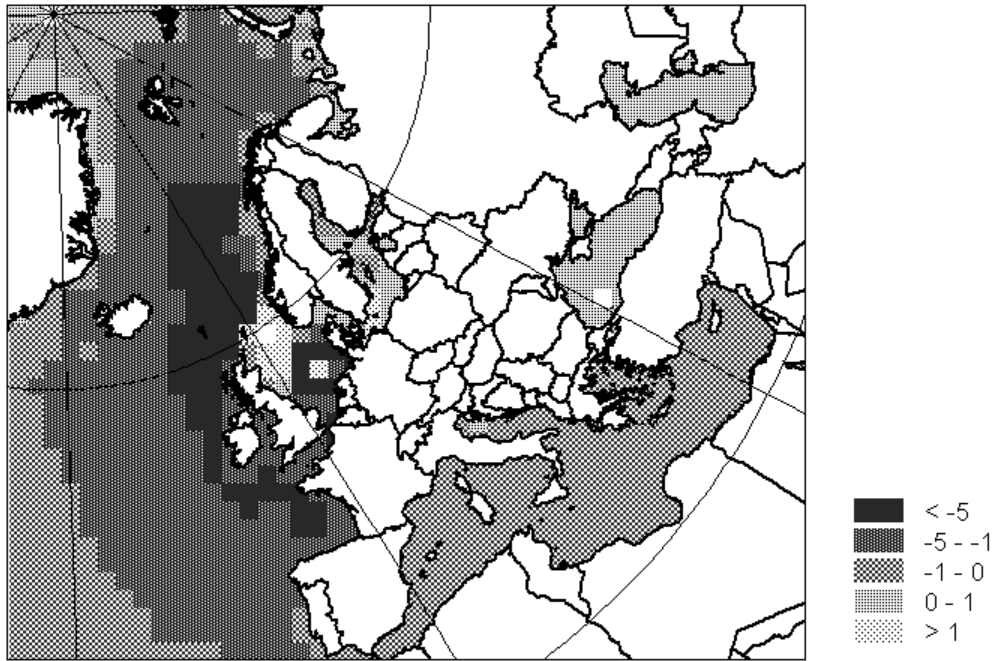
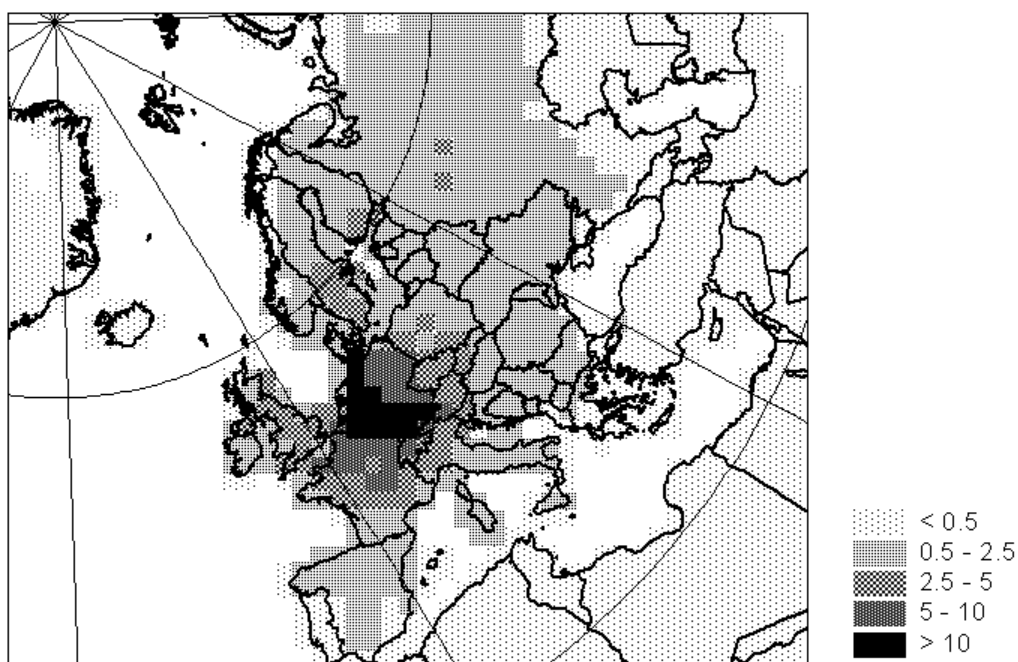**Figure 4.**   Concentration difference in the upper ocean layer, MDO-OSO models, ng/m³

Figure 5.   Variations of concentrations in the upper ocean layer due to advective transport with sea currents, MDO-MDO0 models, ng/m³

As evident from the figure, the introduction of advection in sea water affects PCB-153 concentration in the upper surface layer. The concentration increase (by about 5%) is observed along the coastal line of Scandinavia and Greenland. At the same time in the southern regions of EMEP grid PCB-153 concentrations in the upper layer decrease. These variations obviously are connected with the transport to the north-east in the northern part of the Atlantic. The concentration elevation in the vicinity of southern Greenland coast is caused by Eastern-Greenland current directed to the south-west.

In other environmental compartments (air and soil) the introduction of POP transport processes in the ocean inflicts less impact.

PCB-153 concentrations in the upper soil layer in the OSO experiment are demonstrated on figure 6. The concentration field variation in the upper soil layer in the MDO experiment versus OSO experiment is shown on figure 7. PCB-153 concentrations in soil decrease in MDO experiment. The most significant variations of concentrations are observed in coastal regions. Along the coastal line of Scandinavia and Ireland these variations reach approximately 10%. In the northern part of Central Europe some growth of pollutant concentrations in soil takes place.

Figure 6. Concentrations of PCB-153 in the upper soil layer, OSO model, ng/g

▓	< -0.1
▓	- 0.1 - -0.01
▒	-0.01 - 0
░	0 - 0.01
░	> 0.01
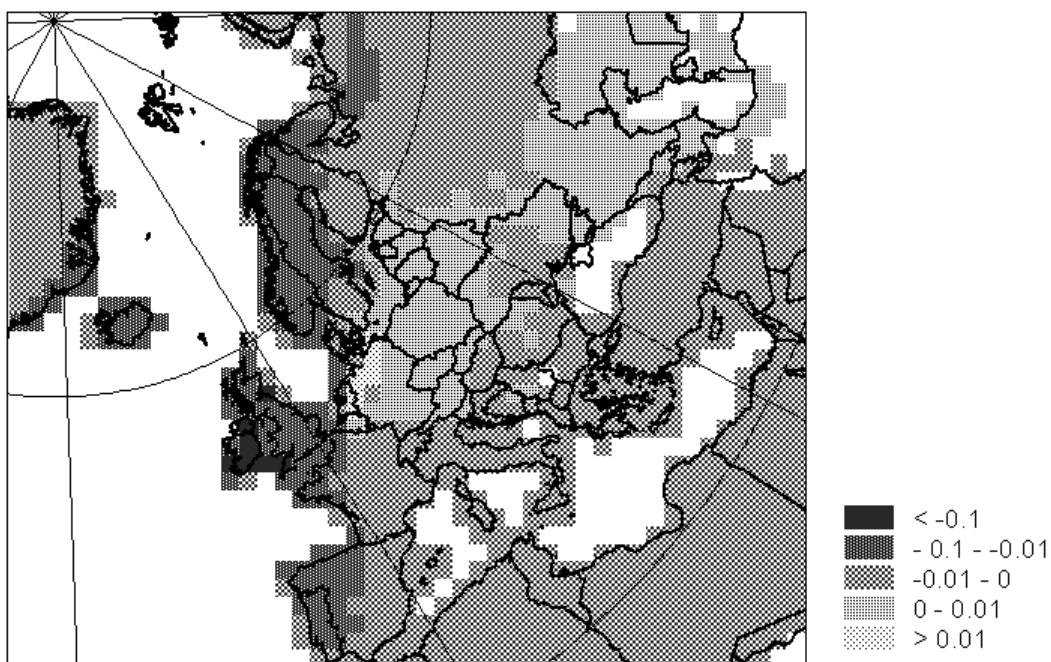
Figure 7.   Concentration difference in the upper soil layer, MDO - OSO models, ng/g

Figure 8 shows PCB-153 concentrations in the lower atmospheric layer in the OSO experiment. Figure 9 illustrates the concentration difference resulted from the introduction of new transport mechanisms in the ocean. Variations, in particular, decrease of concentrations, are mainly observed over the ocean surface.

░	< 0.01
▒	0.01 - 0.1
▓	0.1 - 0.25
▓	0.25 - 0.5
■	> 0.5
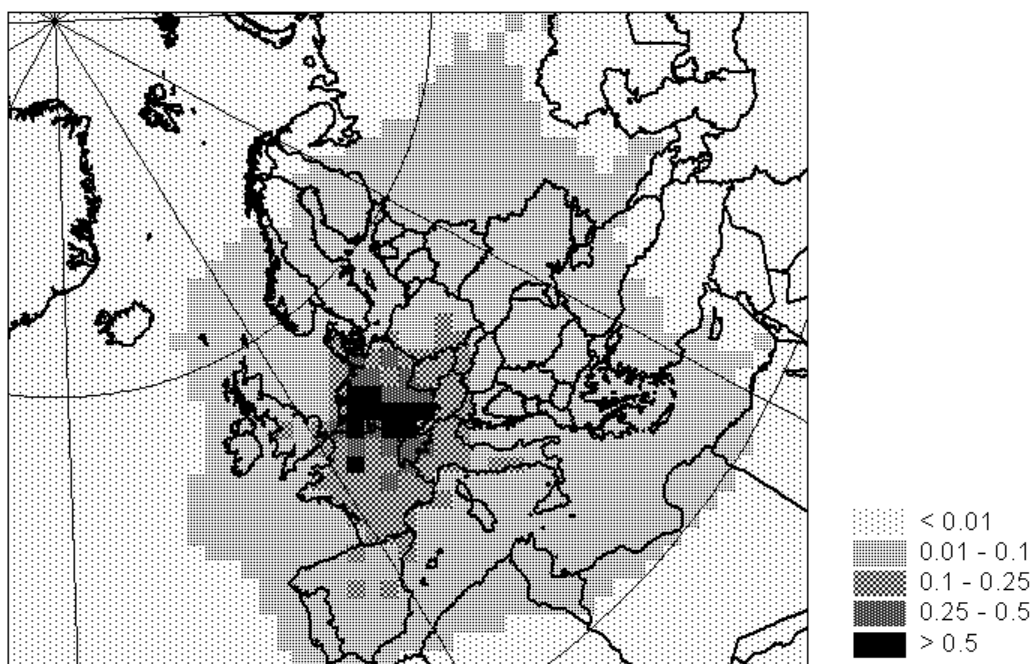
Figure 8.   Concentrations of PCB-153 in the lower atmospheric layer, OSO model, ng/m^3
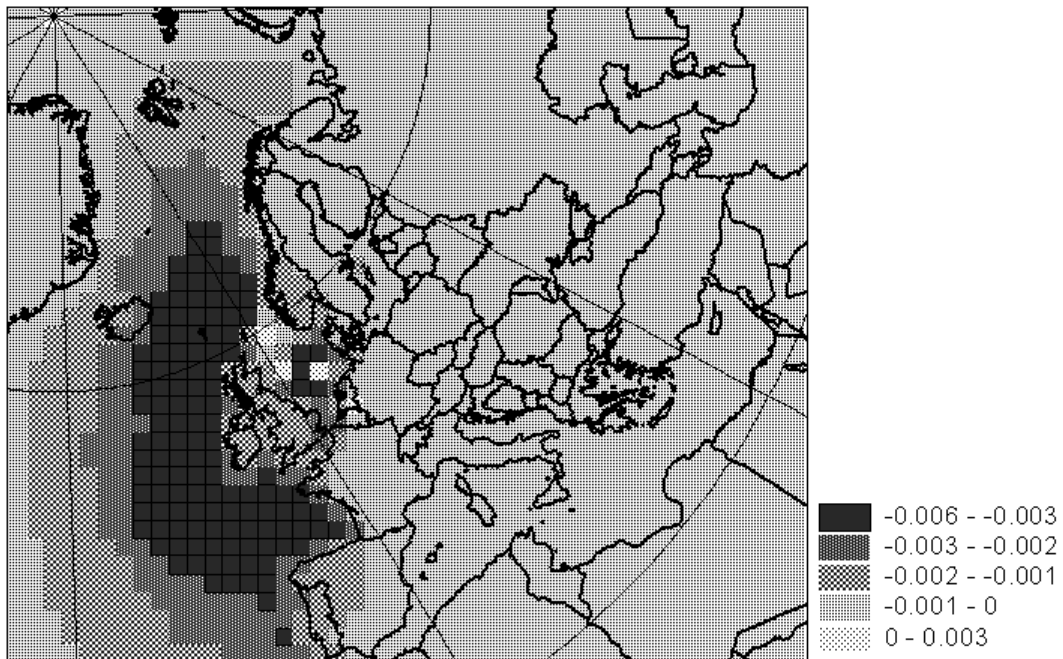
Figure 9.   Concentration difference in the lower atmospheric layer, MDO - OSO models, ng/m^3

Cross section of concentration field along the eastern part of the Atlantic coast in the MDO experiment is shown on figure 10. In the quasi-stationary state of the model POP concentrations decrease with depth. On the northern part of the Atlantic coast the variation with depth is less pronounced. It is explained by the fact that this part of the Atlantic ocean is essentially less deep but mixing of the upper layers is more intensive.
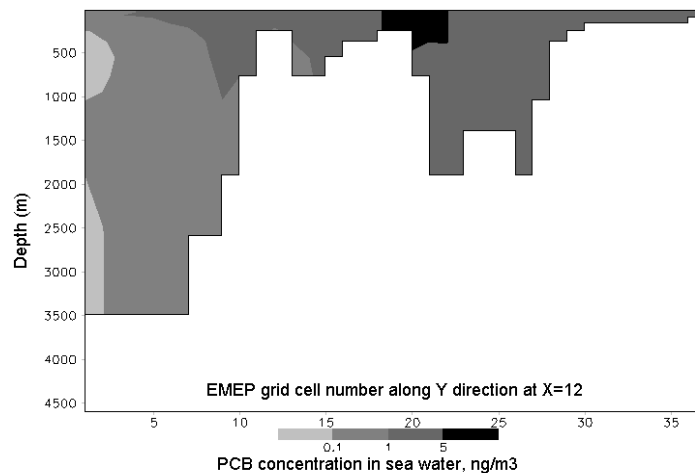
Figure 10.   Vertical distribution of PCB-153 concentrations along the eastern part of the Atlantic coast in the MDO experiment, ng/m^3. Cross section is made along Y direction of the EMEP grid (Figure 1) at X = 12.

PCB-153 mass partitioning between the air and sea water compartments in the MDO experiment differs essentially from that of the OSO experiment.
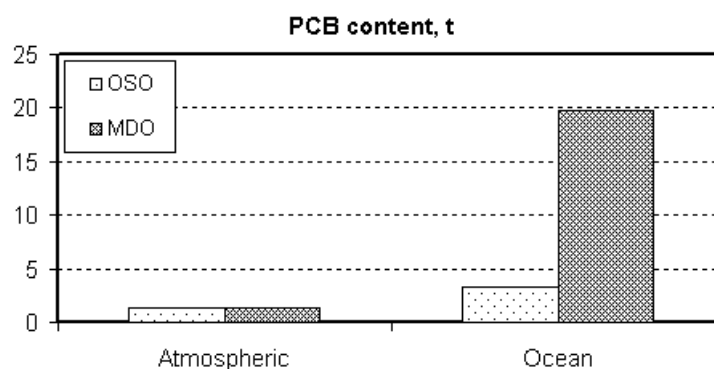
Figure 11. PCB mass partitioning between the atmosphere and ocean in the experiments OSO and MDO in quasi-stationary state after 20 year simulation period

Figure 11 shows values of masses in the atmosphere and ocean for both experiments. As seen from the figure atmospheric PCB-153 mass slightly decreases in the MDO experiment. In the MDO experiment PCB-153 mass is redistributed in such a way that an essentially greater portion of the pollutant is contained in the ocean. Apparently it inflicts a considerable impact on dynamics of pollution distribution with all model compartments and reflects modern ideas that the ocean can accumulate an appreciable amount of POPs.

5. *Comparison of modeling results with measurements*

In order to compare modeling results with measured concentrations of PCBs in ocean the observations carried out under IOC program (Intergovernmental Oceanographic Commission) [*Schulz-Bull et al.,* 1998] were considered. Concentrations of 23 PCB congeners have been measured at 4 Atlantic stations around Iceland. At each station the observed concentrations decreased with depth. In the majority of measurements concentrations of particle bound PCBs exceeded the concentration in the dissolved phase. It is connected with high concentrations of suspended particulate matter in waters washing Iceland. The following table illustrates some measurement results (1993).

Table 1.   Measured and computed total PCB concentrations in sea water, ng/m^3

Station	Co-ordinates		Depth	PCB observed	PCB computed
	^{0}N	^{0}W	m	ng/m^3	ng/m^3
Irminger Sea					
7	63.67	33.0	50	1.9	2.1
7			100	0.7	2.1
7			1500	0.3	2.0
7			2450	0.3	0.4
Greenland Sea					
12	68.2	22.67	300	2.1	2.1
12			870	0.5	
Norwegian Sea					
13	64.8	6.2	180	11.4	7.1
13			1970	1.0	
Faeroe Bank Channel					
14	61.43	8.40	194	1.8	5.0
14			494	1.4	1.7
14			694	0.8	
14			714	0.8	

Computed PCB concentrations obtained with model, including transport and diffusion in sea water, were compared with measured PCB concentrations [*Schulz-Bull et al.,* 1998]. As it can be seen from the table some of the measured values are not matched by the computed ones. This is due to currently rather rough vertical and horizontal resolution of the model. Results of the comparison show that modeled values are in a good agreement with available measurements in sea water. In addition some correlation can be noted in changing of computed and measured concentrations with depth.

6. *Conclusions*

Further development of multi-compartment POP transport model for the EMEP region has been made at EMEP/MSC-E. The development was focused on sea water compartment and transport of the pollutants with sea currents. New vertical structure of this compartment was introduced. Additional processes, in particular, advective transport with sea currents, turbulent diffusion, and refined description of air-sea exchange processes, depending on the surface wind speed, were added. Preliminary computations were made with the model developed. The results of the modelling experiments considered above allow us to draw the following conclusion:

- Description of pollutant redistribution within sea water using the transport processes (sea currents) and turbulent diffusion leads to noticeable increase of PCB accumulation in this compartment. These results reflect current understanding that oceans can be a major storage medium for some of the POPs. At the same time the modifications made result in decreasing of PCB concentrations in the atmosphere and soil.

- Introduction of advective transport due to sea currents results in variation of pollutant concentrations in sea water. Thus preliminary results indicate increasing of PCB concentrations in the vicinity of Scandinavia and Greenland coast and decreasing of them in the southern Atlantic.

- Modeling results were compared with observations of PCB concentrations in sea water of Northern Atlantic. Results of the comparison show reasonable agreement of computed concentrations with available measurements.

- Further development of POP transport model and, in particular, of its sea water compartment, can be connected with the more accurate description of processes important for coastal zones and regional seas, e.g. the North Sea, the Baltic Sea, the Mediterranean Sea, and the Black Sea.

References

Alban L. and R.Jacques [1999] Simulation of radionuclide dispersion in the Pacific Ocean from Mururoa atoll. *Journal of Applied Chem.*; No.43; pp.31-49.

Bidleman T.F. and L.McConnell [1995] A review of field experiments to determine air-water gas exchange of persistent organic pollutant. Science of the Total Environment (NLD); v.159; pp.101-117.

Duce R.A. [1997] Atmospheric input of pollution to the oceans. Marine Meteorology and Related Oceanographic Activities, v.39.

GESAMP [1989] The atmospheric input of trace species to the World Ocean; GESAMP; World Meteorological Organisation, Geneva, Switzeland; No.38; pp.1-111.

Gonzalez E.A. and P.S.Hill [1998] A method for estimating the flocculation time of monodispersed sediment suspension. Deep Sea Research Part I: Oceanographic Research Papers; v.45; pp.1931-1954.

Green T. and D.F.Houk [1979] The removal of organic surface film by rain. *Limnology and Oceanography* (USA); v.24 ; pp. 966-970.

Guilyardi E. and G.Madec [1997] Performance of the OPA/ARPEGE-T21 global ocean atmosphere coupled model. *Climate Dynamics*; v.13; pp.149-165.

von Hobe M., Kettle A.J. and M.O.Andreae [1999] Carbonyl sulphide in and over seawater:summer data from the northeast Atlantic Ocean. *Atmospheric Environment* (GBR); v.33; pp.3503-3514.

Ibraev R.A., Kiryanov S.V., Kuksa V.I. and I.O.Yumlanov [1997] Modelling of the transport of passive pollutants from the Volga river run-of in the Caspian Sea. Meteorology and Hydrology (RUS), No.8, pp.63-69.

Jilan S. and D.Lixian [1999] Application of Numerical Models in Marine Pollution Research in China. *Marine Pollution Bulletin*; v.39; No.1-12; pp.73-79.

Liss P.S. and L.Merlivat [1986] Air sea exchange rates: introdaction and synthethis. The role of air-sea exchange in geometrical cycling (Ed, P-Buat-Menard); D Riedel Mass; pp.113-127.

Liss P.S. and P.G.Slater [1974] Fluxes of gases across the air-sea interface. *Nature*, v.247;   pp.181-184.

Macdonald G., Holley E.R. and J.S.Gouge [1990] Gas transfer measurements on an ice-covered river.; Air-Water Mass Transfer (Ed. Wilhelms S.C., Gulliver J.S.) Sel.Pap.Int.Symp.Gas Transfer Water Surf.2nd; pp.347-361.

Macdonald R., Bidleman T.F., Muir D., Jantunen L.M. and T.Harner [1999] Arctic mass budget - a look at HCH, toxaphene and PCBs; Workshop on Techniques and Associated Uncertainties in Quantifying the Origin and Long-Range Transport of Contaminants to the Arctic. Reports and Extended Abstracts of Workshop. Bergen, 14-16 June.

Pekar M., Gusev A., Pavlova N., Strukov B., Erdman L., Ilyin I. and S.Dutchak [1998] Long-range transport of selected POPs. Development of transport models for lindane, polychlorinated biphenyls, benzo(a)pyrene. EMEP/MSC-E Report 2/98, Part I.

Pekar M., Pavlova N., Gusev A., Shatalov V., Vulikh N., Ioannisian D., Dutchak S., Berg T. and A.-G. Hjellbrekke [1999] Long-range transport of selected persistent organic pollutants. Development of transport models for polychlorinated biphenyls, benzo[a]pyrene, dioxins/furans and lindane Joint report of EMEP Centres: MSC-E and CCC, EMEP/MSC Report 4/99.

Perianez R. and J.Reguera [1999] A numerical model to simulate the tidal dispersion of radionuclides in the English Channel.;Environmental Radioactivity; v.43 ; pp.51-64.

Perianez R. [1998a] Three-dimensional modelling of the tide-induced dispersion of radionuclides in the sea; *Environmental Radioactivity*; v.40; No.3; pp.215-237.

Perianez R. [1998b] Modelling the distribution of radionuclides in deep ocean water columns. Application to 3H, 137Cs and 239,240Pu; *Environmental Radioactivity*; v.38; No.2;   pp.173-194.

Preller R.H. and A.Cheng [1999] Modeling the transport of radioactive contaminants in the Arctic; Marine Pollution Bulletin; v38; No.2; pp.71-91.

Prifman S.L., Eicken H., Bauch D. and W.F.Weeksn [1995] The potential transport of pollutants by Arctic sea ice; Science of the Total Environment (NLD); v.159 ; pp.129-146.

Schulz-Bull D.E., Petrick G., Bruhn R. and J.C.Duinker [1998] Chlorobiphenyls (PCB) and PAHs in water masses of the northern North Atlantic; Marine Chemistry (NLD); v.61; No.1-2;   pp.101-114.

Schwarzenbach R.P., Gschwend P.M. and D.M.Imboden [1993] Environmental organic chemistry; New-York, McGraw-Hill Book Co., Inc.

Sergeev Yu.N. (ed), Kolodochka A.A., Krummel Hk.D., Kulesh V.P. and O.P. Savchuk [1979] Modelling of substance transport and transformation processes in the sea; Modelling of substance transport and transformation processes in the sea. L., published by Leningrad State University, p. 291.

Strand A. and O.Hov [1996] A model Strategy for the Simulation of Chlorinated Hydrocarbon Distribution in the Global Environment. *Water, Air and Soil Pollution,* v.86, pp.283-316.

Waldichuck M. [1982] Air-sea exchange of pollutants; Pollutant Transfer and Transport in the Sea (ed. Kullenberg G.) Boca Raton, Fla.: CRC Press; v.1, pp.178-219.

Wallberg P. and A.Andersson [1999] Determination of adsorbed and absorbed polychlorinated biphenyls PCBs in seawater microorganisms; Marine Chemistry (NLD); No.64; pp.287-299.

Wania F. and D.Mackay [1999] The evolution of mass balance models of persistent organic pollutant fate in the environment. *Environmental Pollution.* a,b (GBR); No.100; pp.223-240.

Wania F., Axelman J. and D.Broman [1998a] A review of processes involved in the exchange of persistent organic pollutants across the air&sea interface; *Environmental Pollution*. a,b (GBR); v.102; No.1; pp 3-23.

Wania F., Hoff J., Jia C.Q. and D.Mackay [1998b] The effects of snow and ice on the environmental behaviour of hydrophobic organic chemical. *Environmental Pollution.* a,b (GBR); v.102;   pp.25-41.

WMO [1997] Report and proceedings of the workshop on the assessment of EMEP activities concerning heavy metals and persistent organic pollutants and their further development (Moscow, Russian Federation, 24-26 September, 1996). WMO/TD No.806.

II. Preparation of biannual file of data on three-dimensional structure of sea currents in the north-east Atlantic and adjacent seas

1. *Introduction*

The objective is to prepare a file of data consistent in terms of dynamic parameters describing three-dimensional structure of velocity fields in the oceanic depth and the surface mixed layer depths with allowance for actual data on atmospheric forcing at the ocean surface during 1987 and 1996. Resultant fields of current velocities are intended for numerical experiments of pollutant transport in the marine environment of the EMEP region.

Available oceanographic observations do not allow us to obtain data on the actual current distribution with the water depth.

In the usual practice the assessment of currents in the oceanic depth is made by calculations of the horizontal component of current velocities in geostrophic approximation on the basis of prescribed (climatic) density distribution in the ocean. The velocity fields obtained in such a way have essential shortcomings. In view of modelling the pollutant transport in the ocean they are:

- neglect of barotropic current component;

- neglect of the effect of bottom relief on currents;

- neglect of drift currents generated by winds in the upper layers;

- as a result it is impossible to calculate correctly vertical motions.

Hence it is impossible to obtain the circulation pattern as accurate as it is required for calculations of a pollutant fate. In order to overcome these difficulties motions in the ocean are specified by models describing main oceanic processes. Such models provide three-dimensional fields of motion velocities with allowance made for atmospheric forcing at the ocean surface. Although the accuracy of modelled fields in many respects is insufficient so far, nevertheless the description of ocean circulation by model calculations is most constructive for the time being.

Thus the work is aimed at calculating current velocity fields and the upper ocean mixed layer depth using a modern ocean general circulation model which should consider data on actual atmospheric forcing at the water surface.

This work includes the preparation of relevant information for configuring the ocean circulation model and for calculating current velocity fields. The input data involve the information for constructing the calculation grid (ocean bathymetry, coastline shape) and external fields of atmospheric forcing for the period covered by calculations.

2. *Outline of the ocean general circulation model (OGCM)*

The ocean general circulation model [*Resnyansky, Zelenko*, 1992] which is under development in Hydrometcentre of Russia since the early 1990s is used for calculations of current velocity fields and the surface mixed layer depth. This model is based on primitive equations in the spherical co-ordinate system with conventional approximations (incompressibility, hydrostatics, Boussinesq, "rigid lid"). The dependent variables in the model are current velocity vector, water temperature T, salinity S, derived from T and S, water density ρ, pressure, and a supplementary variable - integral current function introduced for the solution under the condition of "rigid lid".

Finite-difference approximation of original differential equations is made by so-called box method based on balances in elementary volumes formed by contiguous knots of the grid [*Bryan*, 1969]. For advective terms it leads to central differences with averaging of some grid variables on the grid of B type according to the classification by Arakava [*Mesienger and Arakava*, 1979]. In regard to time "leap-frog" scheme complemented by Rober filter [see *Asselin*, 1972] for the suppression of two-step splitting of the solution is applied. The simulated oceanic basin is represented by a set of boxes with horizontal sides $\Delta\lambda$ and $\Delta\varphi$ along the longitude and altitude respectively and vertical step Δz. The $\Delta\lambda$ step is constant, but $\Delta\varphi$ and Δz steps can vary.

The combined boundary problem is solved within the domain bounded by the ocean surface, $z=0$, its bottom, $z = H(\lambda,\varphi)$, and lateral boundaries for which the conditions of no-slip and vanishing heat and salt flows along the normal are specified. In a general case this domain can be multiply connected, it can be divided into individual continents and islands.

In addition to the above mentioned "rigid lid" at the ocean surface components of tangential wind stress $\tau = (\tau_\lambda, \tau_\varphi)$, heat F^T and fresh water F^S fluxes are prescribed. On the shore - no-slip condition and vanishing heat and salt diffusion fluxes normal to the shore. On the bottom – flow round condition and vanishing heat and salt diffusion fluxes through the bottom.

Surface pressure, which cannot be directly calculated from the original equations due to the condition of the "rigid lid", is excluded by the equation for transport stream function ψ. The latter is an elliptic equation of the second order relative to time derivative $\partial\psi/\partial t$. The boundary conditions along the coastal contour are obtained as a consequence of physical conditions of non-flow through this contour. In the case of singly connected domain they are reduced to the prescription of an arbitrary constant, and in the case of multiply connected domain the unknown values for internal contours are found from relevant relationships by "hole relaxation" method [*Semtner*, 1986].

The accepted difference approximation is similar to the schemes described in [*Bryan*, 1969; *Semtner*, 1986]. As it is shown in these papers, it provides the conservation of mass, heat and salt. When there is no turbulent viscosity and external forcing, it also provides the conservation of the total energy of the whole basin.

Small-scale turbulent mixing in the upper water layer is parameterized with integral upper ocean mixed layer model embedded into the circulation model. The embedding algorithm [*Resnyansky and Zelenko*, 1991] includes mixing of water properties (T, S, ρ) within a certain layer, which depth is determined from the equation of turbulent kinetic energy budget. Property redistribution along the vertical is made in such a way, that their overall content in a water column is conserved, and two basic regimes of upper mixed layer evolution (entrainment and detrainment) are separated depending on the relationship between generation and dissipation of turbulent kinetic energy.

One more mechanism of the vertical exchange associated with density convection is parametrized by the standard scheme of "convective adjustment" switched on every time, when hydrostatically unstable combinations of density values in the neighboring water layers are found. In this scheme like in the upper mixed layer model equalization of properties along the vertical is realized but the mixing zone can be at any depth, and it is defined only by the availability of hydrostatically unstable regions on the density profile.

The model is verified in the course of diversified numerical experiments. The results of initial testing under very simple conditions are presented in [*Resnyansky and Zelenko*, 1991, 1992] alongside a detailed description of the model. In further experiments the simulation of ocean climatic circulation and the study of its sensitivity to model parameter variations was made. Seasonal variability with various types of atmospheric forcing was also reproduced including the analysis of mechanisms of seasonal variation hemispheric asymmetry formation, effects of synoptic variations of atmospheric forcing were investigated as well [*Resnyansky and Zelenko,* 1993, 1996, 1999; *Resnyansky and Zelenko*, 1995a, 1995b, 1997].

These experimental results demonstrated the model capability to reproduce quite satisfactory the evolution of the main oceanographic fields. The prescription of real atmospheric forcing with allowance made for a short-term (synoptic) interval of frequency spectrum provides a similar and more realistic pattern of the oceanic circulation than in the case when averaged, climatic, surface fluxes are prescribed.

3. *The configuration of ocean general circulation model for three-dimensional structure of currents in the EMEP region*

3.1. Calculation domain and model grid

While designing the model of ocean general circulation for a specific problem, the selection of spatial resolution (grid region) is a key problem. In order to provide adequate description of the synoptic part of the oceanic motions spectrum important in respect of energy, horizontal grid steps should be about 10-100 km. Global models with such a resolution require huge computer resources. Therefore for calculating currents it is common to use the calculation domain for a smaller region covering the World Ocean area of interest. Difficulties emerge when we formulate boundary conditions at water boundaries of the selected domain. The simplest way out – to substitute liquid boundaries for "a wall" with boundary conditions similar to those formulated for the coastal line. To avoid distortions of the circulation pattern the walls should be as far as possible from the calculation domain. Thus designing of the model grid is reduced to a compromise between high spatial

resolution, available computer resources and in the case of a regional calculation domain - sufficient distance from fictitious boundaries.

From the above reasoning calculations of currents in the EMEP region were carried out over the model grid containing 152x116x15 knots along the longitude, latitude and depth respectively. In regard to geography this region (34°S-80°N; 99°W-51°E) covers the North Atlantic and an appreciable part of the South Atlantic.

The oceanic depth is divided into 15 layers of different thickness (figure 1). The vertical grid steps grow monotonously from the top to the bottom in conformity with typical distribution of temperature and salinity gradients in the ocean.

The horizontal grid-size (constant and the same along the latitude and longitude) is 1°, i.e. about 100 km in low latitudes and about 50 km in latitude 60°. The selection of this value is conditioned by the available computer resources, projected time-schedule of calculations, as well as it is dictated by spatial scales (50-150 km) of pollutant dispersion processes which are to be investigated by means of calculated current velocity fields.

The horizontal configuration of the grid is shown in figure 2 (the upper map). The location of the coastal line, continent and island outlines correspond to climatic electron atlas WOA-94 [*Levitus et al.*, 1994]**,** which is also used for calculating initial fields of temperature and salinity and which has 1° horizontal resolution exactly coinciding with the model one.

For the same reasons it was convenient to compile files of bottom relief in accordance with field presentations in atlas WOA-94. The resultant ocean depths are shown in figure 2. The calculation region contains all important large-scale bathymetric peculiarities of the Atlantic Ocean: main depressions, rising and ridges.

In a given configuration the calculation region turned out to be triply connected. The internal closed boundary contours (used for calculating constant values of the transport stream function) are formed by the coastal lines of Iceland Island and by an idealized island situated on the location of Cuba and Haiti Islands.

It should be noted that the calculation domain limited in the north by 80°N does not completely cover the EMEP grid (117x111), which includes the circumpolar region. It is connected with the fact that while approaching the pole, linear step decreases consequently the time step is appreciably reduced thereby increasing drastically the computation time.

Besides the description of currents in the near pole region requires to consider ice processes, which are not included in the model for the time being.

<u>*OCEAN MODEL VERTICAL DISCRETIZATION*</u>

```
****************** B=    .00
LEVEL 1  -----Z= 12.50          DZK( 1) =  25.00
****************** B= 25.00
LEVEL 2  -----Z= 37.50          DZK( 2) =  25.00
****************** B= 50.00
LEVEL 3  -----Z= 65.00          DZK( 3) =  30.00
****************** B= 80.00
LEVEL 4  -----Z= 105.00          DZK( 4) =  50.00
****************** B= 130.00
LEVEL 5  -----Z= 165.00          DZK( 5) =  70.00
****************** B= 200.00
LEVEL 6  -----Z= 250.00          DZK( 6) = 100.00
****************** B= 300.00
LEVEL 7  -----Z= 375.00          DZK( 7) = 150.00
****************** B= 450.00
LEVEL 8  -----Z= 550.00          DZK( 8) = 200.00
****************** B= 650.00
LEVEL 9  -----Z= 775.00          DZK( 9) = 250.00
****************** B= 900.00
LEVEL 10  -----Z=1050.00          DZK(10) = 300.00
****************** B=1200.00
LEVEL 11  -----Z=1400.00          DZK(11) = 400.00
****************** B=1600.00
LEVEL 12  -----Z=1900.00          DZK(12) = 600.00
****************** B=2200.00
LEVEL 13  -----Z=2600.00          DZK(13) = 800.00
****************** B=3000.00
LEVEL 14  -----Z=3500.00          DZK(14) =1000.00
****************** B=4000.00
LEVEL 15  -----Z=4600.00          DZK(15) =1200.00
****************** B=5200.00
```

Figure 1.   Ocean model vertical discretization. The scheme shows depths *Z*, layer thickness *DZK* and depths of layer boundaries *B* (indicated by asterisks). All values are given in meters
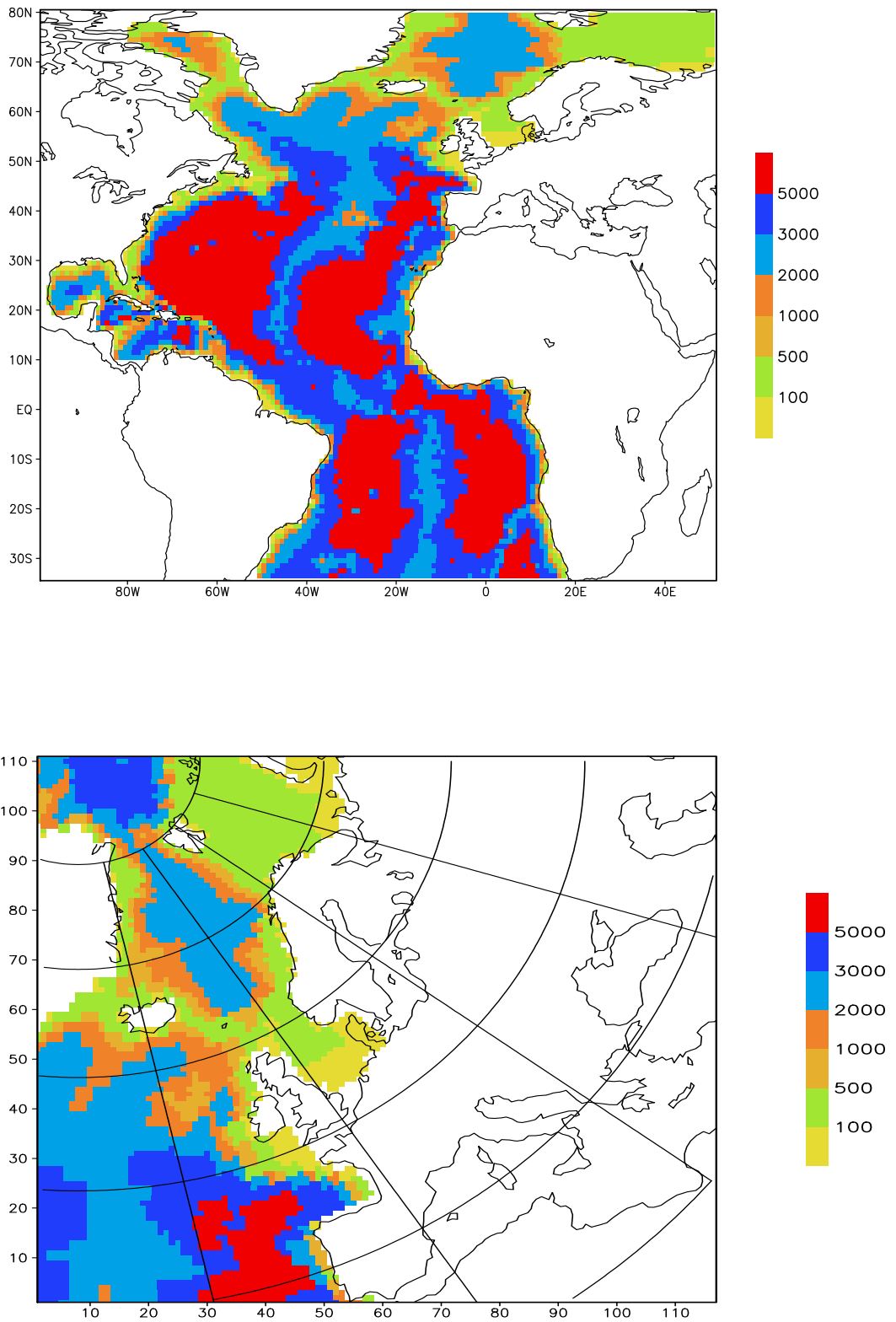
Figure 2. Horizontal configuration of OGCM model grid (the upper map) and of POP transport model grid (the lower map) with bottom relief (m) for both modelling domains

3.2. *Tuning of the model parameters*

The ocean general circulation model includes several physical and algorithmic parameters which values depend first on the difference grid features and second they affect the computation efficiency. Theoretical considerations provide rather general recommendations in regard to values of these parameters. More accurate values can be obtained by tuning numerical experiments.

The first cycle of experiments short in time (several days) was fulfilled for the selection of turbulent exchange coefficients. The overestimation of these coefficients results in smoothing of calculated fields and circulation weakening. When they are underestimated groundlessly it gives rise to numerical instability. As a result of calculations performed the following coefficients were selected:

10^{-3} **m^2/s** - vertical turbulent viscosity coefficient,

10^{-4} **m^2/s** - vertical turbulent diffusion coefficient,

10^{4} **m^2/s** - horizontal turbulent viscosity coefficient,

10^{3} **m^2/s** - horizontal turbulent diffusion coefficient.

The second experimental series more prolonged in time (several months) was aimed at tuning the parameters for the solution of elliptic problem concerned with calculations of transport stream function by the method of sequential upper relaxation. At the same time the optimization of the time step dependent on these parameters was made. Hence in further computations the time step was **30 min** and the upper relaxation parameter was equal   to **1.1** (at convergence criterion relative to residual function of the right part **10^{-3}**).

4. *Formulation of atmospheric forcing at the ocean surface*

In accordance with the model formulation for the ocean surface the second kind conditions are prescribed. These conditions define atmospheric forcing $\tau=(\tau_\lambda,\ \tau_\varphi)$, F^T and F^S dependent on horizontal co-ordinates and time. At the first stages of ocean model development usually these forcing was specified by climatic or at best by mean monthly data. With the advent of systems capable to operate with meteorological data, lack of actual data on some meteorological elements is compensated for those calculated by atmospheric models based to this or that extent on observations. Since that time numerical files on atmospheric ~~impacts~~

---

forcing characterizing current state of energy exchange on the water-air interface have become available for modellers of the ocean. One of the first files which received wide recognition were included to TOGA CD-ROM data set [*Finch*, 1994] compiled in the course of TOGA international experiment. This data set covers the time period 1985-90 and in particular includes wind stress fields prescribed on the global grid with time-step 6 hours and heat flux components provided by European Centre for Medium Range Weather Forecast (ECMRWF). Similar data sets for more prolonged periods were created under the project on the re-analyses of meteorological data. For calculations of currents in this study we used the data set prepared by the US National Centre of Environment Prediction (NCEP), (former National Meteorological Centre (NMC) in collaboration with National Centre for Atmospheric Research (NCAR) [*Kalnay et al.*, 1996].

This data set includes mean daily data on heat flux components (short-wave and long-wave solar radiation, sensible and latent heat fluxes), components of tangential wind stress (τ_λ, τ_φ) and precipitation intensity. All the fields are given on the global geographic grid (192x94 knots) with spatial resolution about 1.9^0 along longitude and latitude. Numerical experiments with the ocean model sampling of required fields for 1986, 1987 and 1996 has been made. Using these data the net heat flux through the water surface (the sum of four components mentioned above) and fresh water flux (the difference between evaporation rate associated with latent heat flux and precipitation intensity) were calculated. In the course of integration by the ocean model the atmospheric forcing were re-interpolated from the original global grid to the grid knots of the calculation model. Updating of data on atmospheric forcing during the integration was made once round the clock in line with input data time temporal discreteness.

5. *Numerical experiment scheme*

The ocean general circulation model used for calculations of the output data on the three-dimensional structure of sea currents is based on evolution equations. For their integration over specific time intervals it is necessary to prescribe initial conditions. Since available experimental data do not allow us to formulate a full set of initial conditions, their acquisition is reduced to provisional integration, to so-called model "spin-up" based on some artificial initial data. The resultant data on oceanographic field states are taken as initial conditions of subsequent calculation series. This scheme is used in the majority of ocean current

computations including problems of pollutant transport [see for example, *Preller and Cheng*, 1999].

The initial condition of the model spin-up represents rest (zero current velocity) with climatological distributions of temperature and water salinity taken from atlas WOA-94 [*Levitus et al.*, 1994; *Levitus and Boyer*, 1994]. The spin-up covered the time period of one year and for atmospheric forcing daily data on heat fluxes, fresh water fluxes and tangential wind stress for 1986 were used.

The resultant state formed by the late 1986 was the starting point of the output data on three-dimensional structure of currents and the upper mixing layer depth. These data were calculated for two sequential time intervals, 1987 and 1996, with appropriate supply of daily atmospheric forcing to the ocean model. Some artificial violation of the natural chronology (abrupt transition from 1987 to 1996) should not appreciably affect the evolution of currents in surface layers. Here wind component prevails, which characteristic evolution time does not exceed several days [see, for example, *Zhukov*, 1976]. For deep water layers with greater thermal and dynamic inertia the consequences can be more essential. However, to obtain estimates of pollutant redistribution in the ocean for lasting time periods (about a year or more) individual peculiarities of specific current systems are not of main significance, and a key role plays statistics of their sequential states produced by atmospheric ~~impacts~~ forcing. For example, in the paper [*Preller and Cheng*, 1999] mentioned above in calculations of radioactive species transport wind fields averaged over 1986 and 1992 were used.

6.   *Transformation of data to the EMEP grid*

As the EMEP region a rectangular domain in the plane of polar stereographic projection (section along 60°N) with angles in the following geographic co-ordinates: (λ=324.32^o, φ=40.65^{o}N), (λ=13.00^o, φ=24.08^{o}N), (λ=229.87^o, φ=86.59^{o}N), (λ=58.53^o, φ=40.74^{o}N) is considered. Axis y is directed in parallel with meridian 328°. The grid with gridsize 50 km in latitude 60° contains 117 knots along axis *x* and 111 knots along axis *y*. The pole location coincides with the grid knot (8,110).

This region covers the north-east Atlantic, the North, Norwegian, Greenland, Barents seas and part of the North Polar basin. Inland seas (the Mediterranean, Baltic, White, Black,

---

Caspian seas) located also in this region were not considered since the horizontal spatial resolution of 1°x1° is not sufficient for an accurate description of motions in relatively small marine basins. The circumpolar region to the north of 80°N was excluded as well since it requires a special procedure for the consideration of strong convergence of meridians in the model spherical co-ordinate system.

When calculating fields in the required stereographic grid the basic problem is connected with the fact that for reasons discussed above the model grid, for which current velocity fields and mixed layer depths are computed, does not cover completely the EMEP region. Therefore additional considerations are needed for the prescription of required values in circumpolar region.

As far as the upper mixed layer (UML) is concerned it is justified to use the minimum value for it since this part of the region is covered by ice over the whole year screening ocean/atmosphere heat exchange thereby establishing stratification close to neutral or stable one. Therefore UML depth is not calculated and it is accepted to be equal to the depth of the first model layer (25 m). UML for the rest of the region is calculated by bilinear interpolation from the model grid.

In contrast to UML scalar value the conversion of horizontal velocity vector is more complicated due to lack of a priori substantiated ideas on the velocity field in this region. Based on modern knowledge that this region is free from pronounced strong ocean currents it is most reasonable to assume zero velocities for this small part of the resultant grid. For the remained part of the EMEP grid velocity values are determined in two steps. At first using bilinear interpolation velocity components were converted from the model grid to the stereographic grid knots. Then velocity vector was converted from the geographical co-coordinate system $[u_g, v_g]$ to stereographic one $[u_s, v_s]$. The process is reduced to turning the obtained velocity vector over some angle, which value depends on geographic longitude (λ):

$$u_s = u_g \cos(\lambda\text{-}328°) - v_g \sin(\lambda\text{-}328°),$$

$$v_s = v_g \cos(\lambda\text{-}328°) + u_g \sin(\lambda\text{-}328°)$$

The fields of velocity components u_s, v_s obtained in such a way for all 15 layers were put to the file described later (section 8) which together with the file of UML depth values constitutes the resultant file.

7.   *Illustrations of calculated fields*

To exemplify resultant fields of current velocities figure 3 demonstrates horizontal velocity vector distribution at depths 65 and 550 m for January 1, 1996. These distributions are characteristic of other periods of time, since the most powerful systems of ocean currents in the water depths below the upper layer are subjected to rather moderate variations in time.

It is evident that in the velocity field for the upper layer the main currents of the North Atlantic are detected: North Atlantic, Irminger, Eastern Greenland, Norwegian, Western Spitsbergen and others. At the depth 550 m current velocities are noticeably slow, and most distinct circulation is observed along Farero-Shetland rising. In the north of the region in the separated collapse basin currents are weak and have no distinct structure.

In the upper ocean layer subjected to drastic variability due to synoptic fluctuations of atmospheric forcing at the oceanic surface, current structures can be detected by fields averaged over some time.

Figure 4 illustrates fields at the depth of the mixed layer for January and July 1996. In winter mixing takes place in deep waters sometimes reaching the bottom. It happens due to convective processes conditioned by severe cooling on the ocean surface. The model adequately represents the location of deep water formation and associated processes important in the context of long-term pollutant dispersion. In summer the character of heat exchange with the atmosphere changes, and the ocean receives heat from solar radiation. Therefore stratification of the upper layers is stable, that is reflected in low values of the upper mixed layer depth (figure 4). Some regions of its deepening are connected with enhanced wind mixing in storm areas.
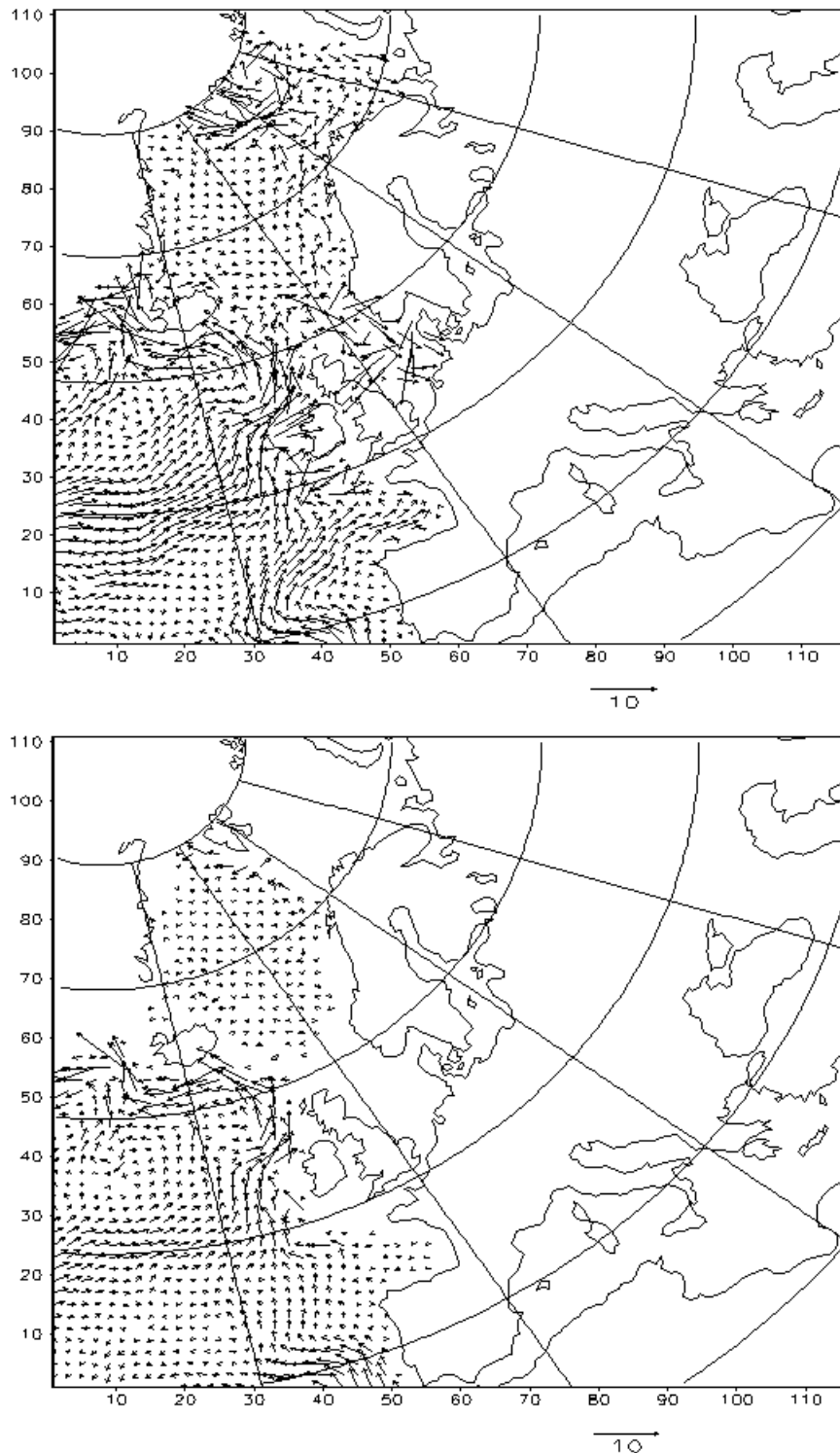
Figure 3.   Horizontal velocities (cm/s) at depth 65 and 550 m for January 1, 1996
in the EMEP stereographic grid

For pictorial presentation the figure demonstrates vectors for a thinned out grid
(in a knot).
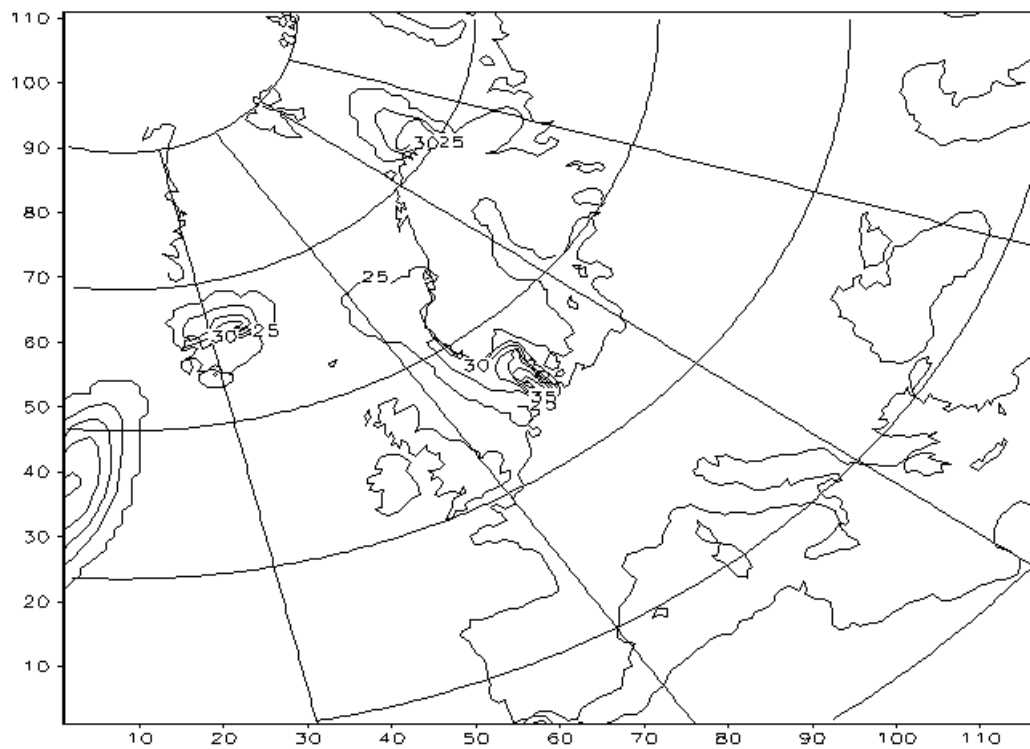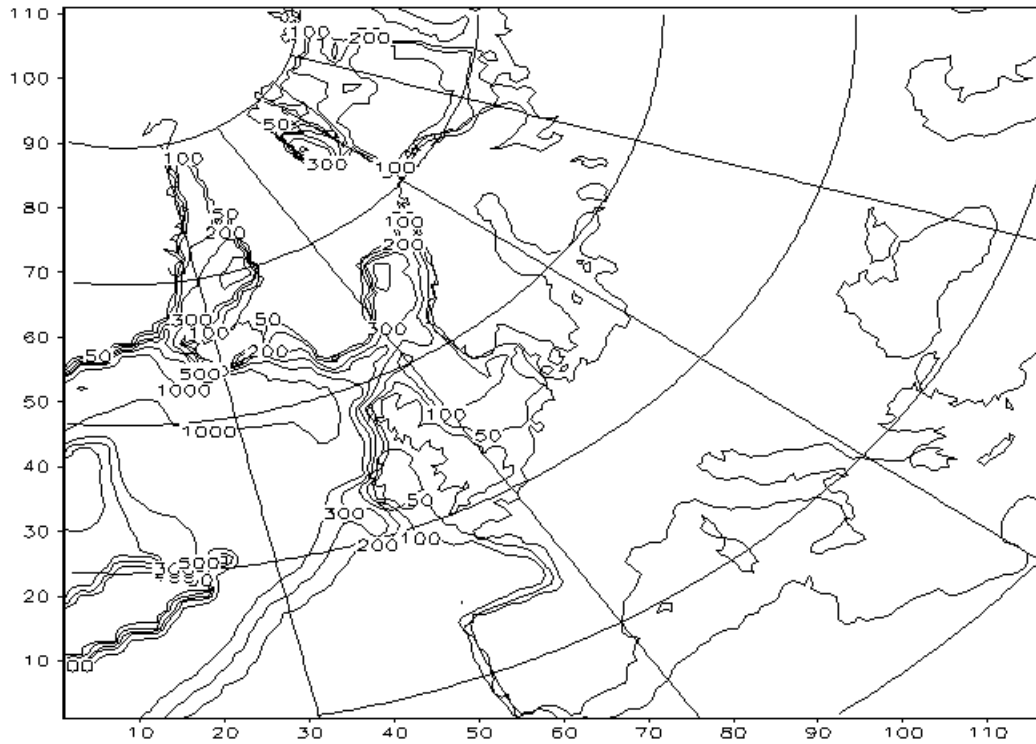
Figure 4.   Isolines of distribution of mixed layer depths (m)
                        for January (the upper map) and July (the lower map) 1996

References

Asselin R. [1972] Frequency filter for time integration. *Monthly Weather Rev.*, v.100, No.6, p.487-490.

Bryan K. [1969] A numerical method for the study of the circulation of the world ocean. *Comput.Phys.*, v.14, No.3, pp.347-376.

Finch C.J. [1994] TOGA CD-ROM Users' Guide. Physical Oceanography DAAC, JPL, Calif. Inst. Technology, 1994, p.126.

Kalnay E., Kanamitsu M., Kistler R., Collins W., Deaven D., Gandin L., Iredell M., Saha S., White G., Woollen J., Zhu Y., Leetmaa A., Reynolds R., Chelliah M., Ebisuzaki W., Higgins W., Janowiak J., Mo K.C., Ropelewski C., Wang J., Jenne R. and J.Dennis [1996] The NCEP/NCAR 40-Year Reanalysis Project. - Bulletin of the American Meteorological Society, v.77, No.3, pp.437-471.

Levitus S. and T.P.Boyer [1994] World Ocean Atlas 1994, v.4, Temperature. NOAA Atlas NESDIS 4.

Levitus S., Burgett R. and T.P.Boyer [1994] World Ocean Atlas 1994, v.3, Salinity. NOAA Atlas   NESDIS 3.

Mesienger F. and A.Arakava [1979] Numerical methods used in atmosphere models (Translation from English). L., Hydrometeopizdat, p.136.

Preller R.H. and A.Cheng [1999] Modeling the transport of radiactive contaminants in the Arctic. – Marine Pollution Bulletin, v.38, No.2, pp.71-91.

Resnyansky Yu.D. and A.A.Zelenko [1991] Parametrization of the upper mixed layer in an ocean general circulation model. - Izvestiya of the USSR Academy of Sciences. Atmosphere and Ocean Physics, v.27, No.10, pp.1080-1088.

Resnyansky Yu.D. and A.A.Zelenko [1992] Numerical realization of the ocean general circulation with parametrization of the upper mixed layer. Proceedings of the USSR Hydrometcentre, v.323, pp.3-31.

Resnyansky Yu.D. and A.A.Zelenko [1993] Sensitivity studies and climatic ocean circulation modelling. *Meteorology and Hydrology*, No.2, pp.77-86.

Resnyansky Yu.D. and A.A.Zelenko [1995a] Seasonal changes simulated by an ocean general circulation model with imbedded upper mixed layer. *Annales Geophysicae*, part II. Oceans, Atmosphere, Hydrology and Nonlinear Geophysics. Suppl. II to v.13, p.C366.

Resnyansky Yu.D. and A.A.Zelenko [1995b] Hemispheric asymmetry of the seasonal changes in a numerical model of the World Ocean general circulation. International Conference "Dynamics of Ocean and Atmosphere", Moscow, November 22-25, p.38.

Resnyansky Yu.D. and A.A.Zelenko [1996] Seasonal variation of ocean general circulation based on data on numerical modelling with two types of atmospheric forcing. *Meteorology and Hydrology*, No.9 pp.65-74.

Resnyansky Yu.D. and A.A.Zelenko [1997] Hemispheric contrasts in the seasonal variations of ocean circulation as inferred from an ocean GCM. - 1997 Joint Assemblies of the International Association of Meteorology and Atmospheric Sciences and International Association for the Physical Sciences of the Oceans, Melbourne, 1-9 July 1997. Abstracts of papers. Ed. by D. Jasper and T. Beer, pp. JMP1-7-JMP1-7.

Resnyansky Yu.D. and A.A.Zelenko [1999] Effects of synoptic variations of atmospheric forcing in an ocean general circulation model: direct and indirect manifestation. *Meteorology and Hydrology*, No.9 pp.66-77.

Semtner A.J. [1986] Finite-difference formulation of the World Ocean model. - NATO Advanced Study Inst. on Advanced Phys. Oceanogr. Numerical Modeling. Ed. J.J.O'Brien. NATO ASI Ser. v.186. Dordrecht.

Zhukov L.A. [1976] General Oceanology, L., Hydrometeoizdat.